

Understanding the nanoscale structure of hexagonal phase lyotropic liquid crystal membranes

Benjamin J. Coscia Douglas L. Gin Richard D. Noble Joe Yelk
Matthew Glaser Xunda Feng Michael R. Shirts

October 3, 2017

Introduction

Nanostructured membrane materials have become increasingly popular for aqueous separations applications such as desalination and biorefinement because they offer the ability to control membrane architecture at the atomic scale allowing the design of solute-specific separation membranes. [?]

- Most membrane-based aqueous separations of small molecules can be achieved using reverse osmosis (RO) or nanofiltration (NF) [?]

While RO and NF have seen many advances in the past few decades, they are far from perfect separation technologies.

- *RO membranes*
 - Inconsistent performance : Current state-of-the-art RO membranes are unstructured with tortuous and polydisperse diffusion pathways which leads to inconsistent performance [?]
 - High energy requirements : Necessarily high feed pressures drive up energy requirements which strains developing regions and contributes strongly to CO₂ emissions. [?]
 - Separation based on differences in solubility and diffusivity: Moreover, designing RO membranes to achieve targeted separations of specific solutes is nearly impossible because various solutes dissolve into and diffuse through the polymer matrix at different rates. [?]
 - At best, one can exploit these differences to create a functional selective barrier.
- *NF membranes*
 - NF was introduced as an intermediate between RO and ultrafiltration, having the ability to separate organic matter and salts on the order of one nanometer in size.
 - Larger and well-defined pores drive down energy requirements while still affording separation of solutes as small as ions to some degree [?]
 - NF is often used as a precursor to reverse osmosis
 - Unfortunately, NF membranes, like RO, possess a pore size distribution which limits their ability to perform precise separations [?]

Nanostructured membranes can bypass many of the performance issues which plague traditional NF and RO membranes.

- Tune size and functionality of building blocks to control pore size and shape: One can accomplish targeted separations with high selectivity by tuning shape, size and functionality of the molecular building blocks which form these materials.

- As a result, solute rejecting pores can have their sizes tuned uniformly, resulting in strict size cut-offs.
- Entirely different mechanisms may govern transport in a given nanostructured material which can inspire novel separation techniques.

Development of nanostructured materials has been limited by the ability to synthesize and scale various fundamentally sound technologies.

- Graphene sheets are atomically thick which results in excellent permeability but defects during manufacturing severely impact selectivity. [?]
- Molecular dynamics simulations of carbon nanotubes show promise [?] but synthetic techniques are unable to achieve scalable alignment and pore monodispersity.[?, ?]
- Zeolites have sub-nm pores with a narrow pore size distribution and MD simulations exhibit complete rejection of solvated ions, [?] however, experimental rejection was low and attributed to interstitial defects formed during membrane synthesis [?]
- There is a need for a scalable nanostructured membrane

Self assembling lyotropic liquid crystals (LLCs) are a suitable candidate for aqueous separation applications.

- LLCs share the characteristic ability of nanostructured membrane materials to create highly ordered structures with the added benefits of low cost and synthetic techniques feasible for large scale production [?]
- Neat liquid crystal monomer forms the thermotropic, Col_h phase. The presence of small amounts of water results in the H_{II} phase.
- In both cases, monomers assemble into mesophases made of hexagonally packed, uniform size, cylinders with hydrophilic groups oriented inward towards the pore center and hydrophobic groups facing outward.
- H_{II} and Col_h phase systems created by the monomer named Na-GA3C11 has been extensively studied experimentally [?, ?, ?, ?, ?].
- Until recently, mesophases formed by Na-GA3C11 could not be macroscopically aligned, resulting in a low flux membrane, slowing research in the field.
- In 2014, Feng et al. showed that the mesophases could be aligned using a magnetic field with subsequent crosslinking to lock the structure in place [?]
- In 2016, Feng et al. showed that the same result could be obtained using a technique termed soft confinement [?].
- Following this breakthrough, research into LLC membranes has been reinvigorated

A molecular level understanding of LLC membrane structure, enabled by molecular dynamics simulations, will provide guidelines to reduce the large chemical space available to design monomers for creation of separation-specific membranes.

- Over the past 20 years, HII phase LLC membrane studies have been limited primarily to Na-GA3C11 with some characterization done after minor structural modifications [?].
- Rejection studies show that this membrane can not perform separations of solutes less than 1.2 nm in diameter because the pores are too large [?].
- We do not yet understand how to reduce the effective pore size or how to tune the chemical environment in the nanopores for effective water desalination or small organic molecule separations.

- It will be challenging to efficiently narrow down the large design space in a laboratory setting without a robust model.
- The only source of predictive modeling has been macroscopic models which likely do not adequately describe transport at these length scales.
- Choice of head group may play a role in the rejection of charged or uncharged solutes.
- Choice of counterion may influence the establishment of a Donnan potential affecting the degree to which the membrane can exclude charged species.
- A good molecular model should incorporate a detailed picture of the nanoscopic pore structure which will be crucial to understanding the role of monomer structure in membrane design.
- Molecular dynamics will have the required level of detail

Our approach to constructing a general model will follow the development of a model of a specific LLC membrane with sufficient experimental characterization.

- We have chosen to focus on assemblies formed by Na-GA3C11
- We have also narrowed our scope to the development of a model of the Col_h phase membrane.
- Compared to the H_{II} phase, the Col_h phase is a simpler starting point, due to the absence of water, and has equivalent experimental structural data.
- Despite having structural data, there is still information which experiment cannot definitively answer.

Despite having structural data, there is still information which experiment cannot definitively answer. There are several key questions that we intend to answer which will be laid out and numbered in subsequent paragraphs.

Monomers in the Col_h system are theorized to be partitioned into stacked layers which form columnar pores. There has been no definitive answer in literature regarding the number of monomers in each layer. We want to know (1) If layers do exist, how many monomers constitute a single layer?

- A simple molecular simulation study of a similar molecule suggested that there are 4 monomers in each layer. Their estimation is based on a simulated system containing only 16 total monomers which likely does not sufficiently model the chemical environment present in the real system. [?].
- A separate calculation based on the volume of the liquid crystal monomers proposes that there are seven monomers in each layer [?].
- A molecular model orders of magnitude larger than any other reported atomistic liquid crystal membrane simulations has the best chance of directly answering this question.
- We can directly change the layer composition and note its effect on membrane structure.

(2) Does our model support the existence of layers and if so, how well defined are the layers?

- Experimentally, their existence is supported by evidence of strong π - π stacking interactions in the direction perpendicular to the membrane plane.
- π - π stacking will only occur between monomer head groups which leaves no description of what is happening in the monomer tail region
- The tails may entangle isotropically while stacking order is maintained among headgroups.

(3) How do monomers in each layer position themselves with respect to surrounding layers?

- A driving force of self assembly in this system is thought to be π - π stacking interactions between aromatic headgroups [?].

- Gas phase ab initio studies of benzene dimers have shown a clear energetic advantage for parallel displaced and T-shaped π - π stacking conformations versus a sandwiched conformation [?].
- Substituted benzene rings exhibit an even stronger π - π stacking attraction which favors the parallel displaced configuration in all cases except where the substitutions are extremely electron withdrawing [?, ?].
- We can use simulated X-ray diffraction patterns to compare the two stacking configurations.

(4) Can the system exist in other metastable states or phases that are not accessed during experiments? There remains the possibility that there is more than one metastable state associated with a given LLC system.

- Simulating a membrane atomistically will require many atoms which further limits the timescales accessible with MD
- It is reasonable to expect that we will generate configurations which are kinetically trapped in a metastable free energy basin
- We must be able to identify which state is produced experimentally and why others are not.

Once we have addressed all of the above questions, we must show that the developed molecular model is consistent with physical observations so that we can rely on conclusions drawn about structural features characteristic of the system.

- In this study, we build a significantly more realistic atomistic model of LLC membranes than has ever previously been done, and explore what new structural information can be gained and what structure hypotheses are supported by this model.
- We validate the model using as much experimental information as possible.
- We are most interested in reproducing the conclusions about structure which have been made from X-ray diffraction (XRD) experiments and in matching ionic conductivity measurements [?].
 - We have compared simulated X-ray diffraction patterns to experiment in order to match major features present in the 2D patterns.
 - We calculated ionic conductivity using two agreeing methods.
 - We examined the influence of crosslinking on membrane structure.
- The structure-building approach and analysis used in this paper can be readily extended to the H_{II} phase and other similar LC systems.

Methods

Liquid crystal monomers were parameterized using the Generalized AMBER Forcefield [?] with the Antechamber package [?] provided with AmberTools16 [?]. Atomic charges were assigned using tools from Openeye Scientific Software. All molecular dynamics simulations were run using the latest version of Gromacs 2016. [?, ?, ?, ?]

An ensemble of characteristic, low-energy vacuum monomer configurations were constructed by applying a simulated annealing process to a parameterized monomer.

- Monomers were cooled from 1000K to 50K over 10 nanoseconds.
- A low energy configuration was randomly pulled from the trajectory and charges were reassigned using the am1bccsym method of molcharge shipped with Openeye Scientific software's QUACPAC
- Using the new charges, the monomer system was annealed again and monomer configurations were pulled from the trajectory to be used for full system construction (Figure 1a).

The timescale for self assembly of monomers into the hexagonal phase is unknown and likely outside of a reasonable length for an atomistic simulation, calling for a more efficient way to build the system.

- Previous work has shown a coarse grain model self assemble into the H_{II} phase configuration in ≈ 1000 ns [?].
- We attempted atomistic self-assembly by packing monomers into a box using Packmol [?].
- Simulations of greater than 100 ns show no indicators of progress towards an ordered system.
- To bypass the slow self-assembly process, python scripts are used to assemble monomers into a structure close to one of a number of hypothesized equilibrium configurations (Figure 1).

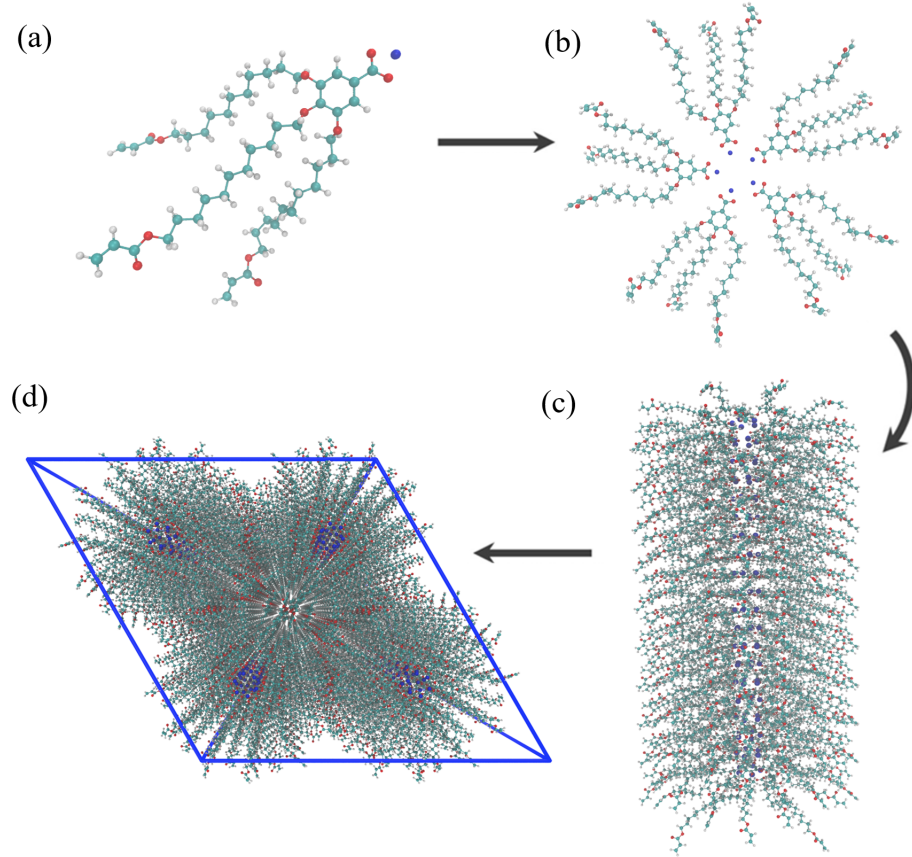


Figure 1: (a) A single monomer was parameterized and annealed to produce a low energy configuration. (b) Monomers are rotated and assembled into layers with hydrophobic centers. (c) Twenty layers are stacked on top of each other to create a pore. (d) Pores are duplicated and placed in a monoclinic unit cell

A typical simulation volume contains four pores in a monoclinic unit cell, the smallest unit cell that maintains hexagonal symmetry when extended periodically.

- Each pore is made of twenty stacked monomer layers with periodic continuity in the z direction, avoiding any edge effects and creating an infinite length pore ideal for studying transport.
- A small number of layers is preferred in order to reduce computational cost and to allow us to look at longer timescales.
- Ultimately, we chose to build a system with 20 monomer layers in each pore in order to obtain sufficient resolution when simulating X-ray diffraction patterns. This point will be explained in more detail later.

- We chose initial guesses for the remaining structural parameters based on experimental data and treated them as variables during model development.

We used experimental wide angle X-ray scattering (WAXS) data (produced as described in [?]) and small angle X-ray scattering (SAXS) data from [?] to inform some of our initial guess choices (Figure 2). We rely primarily on the 2D WAXS data since it encodes all structural details down to the sub-nm scale.

- There are five major features of interest present in the 2D experimental pattern shown in Figure 2b.
- The first is located at $q_z = 1.7 \text{ \AA}^{-1}$, corresponding to a real spacing of 3.7 \AA . The reflection is attributed to $\pi-\pi$ stacking between aromatic rings in the direction perpendicular to the membrane plane, or z-axis [?]. For simplicity, this reflection will be referred to as R- π .
- A weak intensity line is located at exactly half the q_z value of R- π ($q_z = 0.85 \text{ \AA}^{-1}$), corresponding to a real space periodic spacing of 7.4 \AA . This reflection has been interpreted as 2_1 helical ordering of aromatic rings along the z axis meaning if the positions of the aromatic rings can be traced by a helix, then for each turn in the helix, there should be two aromatic rings. For this reason it will be referred to as R-helix.
- A third major reflection is marked by a low intensity ring located at $r = 1.4 \text{ \AA}^{-1}$. The real space separation corresponds to 4.5 \AA which is characteristic of the average spacing between packed alkane chains. This reflection will be called R-alkanes.
- Within R-alkanes, are four spots of higher intensity which will be called R-spots. All are located ≈ 40 degrees from the q_z axis in their respective quadrants. In many liquid crystal systems this can be explained by the tilt angle of the alkane chains with respect to the xy plane.
- The first corresponds to the spacing and symmetry of the d_{100} plane which can be related to the distance between pores. The feature, which will be called R-pores, is characterized by dots along $q_z = 0$. The spacing between dots is indicative of the hexagonal symmetry of the packed pores. The same information at higher resolution is obtained using a SAXS setup. By radially integrating the 2D data one gets a 1D curve which is shown in Figure 2a.

We chose the initial layer spacing based on R- π .

- Each monomer was rotated so the plane of the aromatic head groups would be parallel to the xy plane.
- The layers are placed so aromatic rings are stacked 3.7 \AA apart in the z-direction.
- We extracted the equilibrium distance between layers based on the first peak of a spatial correlation function, $g(z)$, measured along the z-axis (perpendicular to the membrane plane)
- To calculate $g(z)$, we binned the z component distances between the center of mass of each benzene ring and all others of the same pore over 50 ns of equilibrated trajectory and then normalized by the average number density.
- To extract the average distance between layers we applied a discrete fourier transform to the data and extracted the highest intensity frequency
- We compare the degree of layering between systems based on the amplitude of the first peak in $g(z)$. We halve the difference between the maximum of the first peak and the following minimum. We compare the difference to the mean to get a percentage deviation from the average number density.
- Our simulations tend to equilibrate to a wider interlayer spacing of $\approx 4.1 \text{ \AA}$, which inspired separate systems starting with layer spacings greater than 4 \AA .

We placed pores at a chosen initial spacing based on R-pores, then allowed the system to settle into its preferred spacing.

- The model's pore centers are spaced 4.5 nm apart initially, $\approx 10\%$ larger than the experimental value of 4.12 nm in order to reduce unintended repulsions resulting from a tightly packed initial configuration.

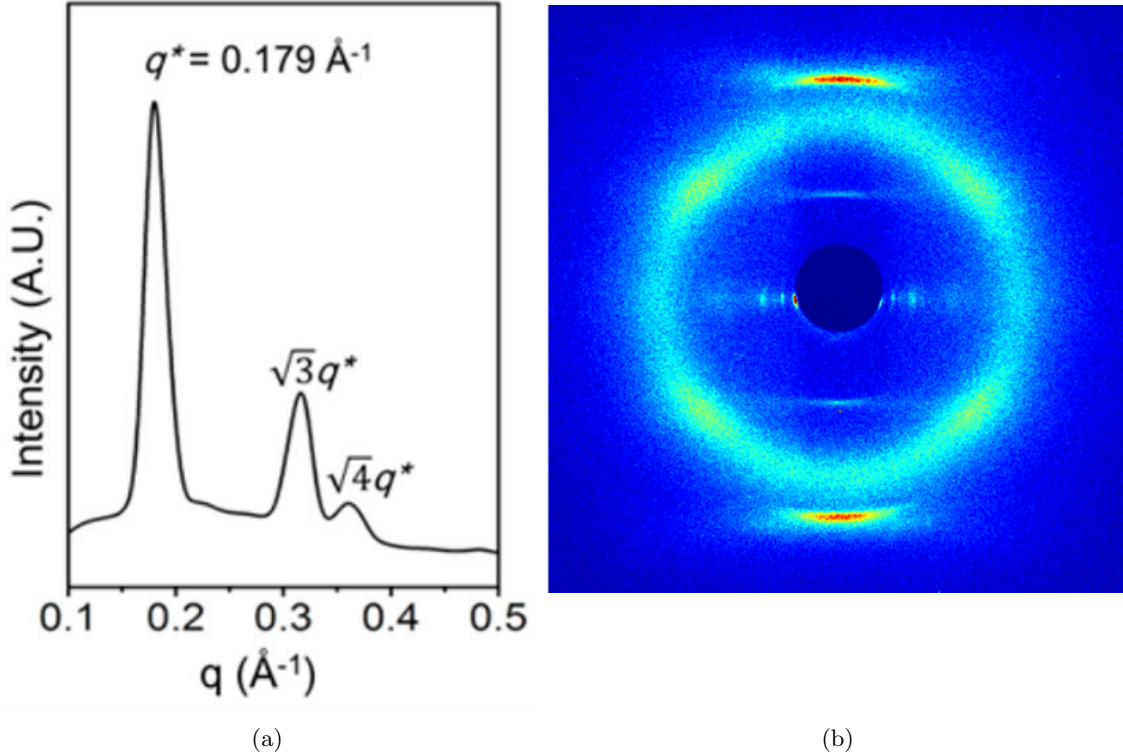


Figure 2: (a) 2D wide angle X-ray scattering gives details about repeating features less than 1 nanometer apart. (b) 1D small angle X-ray scattering indicates hexagonal packing of pores as well as the spacing between pores.

- To calculate the equilibrated pore spacing, we measured the distance between pore centers.
 - Pore centers were located by averaging the coordinates of sodium ions in their respective pores.
 - Statistics were generated using the bootstrapping technique (See Supplemental Information)
 - For each bootstrap trial, we recreate an equilibrium trajectory by randomly sampling from the original trajectory
 - Each pore spacing has its own trajectory with its own average value
 - The average value of each pore spacing is averaged to get the overall average pore spacing.
 - The standard deviation of average values is reported as the uncertainty in pore spacing
 - We are interested in 5 pore-to-pore distances which should all be equal in a perfect hexagonal array. Only 4 are independent

We based the pore radii of our initial configuration on past TEM and size exclusion rejection data. We used experimental Transmission electron microscopy (TEM) and size exclusion rejection data [?, ?, ?] to inform our definition of pore radius in the initial configuration.

- Experimental evidence suggests uniform pores with radii of 0.6 nm
 - Comparing a geometric measurement of pore size derived from an atomistic model, to a less precise, experimentally derived pore size estimate, will give ambiguous results.
 - What is meant by pore radius will not be clear until we establish a clear picture of the nanoscopic pore environment.

- When constructing pores, we chose the carboxylate carbon from the monomer head group as a reference atom, and placed it a distance r from the pore center, where r is the pore radius. (See Supplemental Information)
- We will not make direct comparisons of pore radius between our model and experiment to avoid the ambiguity, however, we do define a pore radius based for our own purposes.
- To measure the pore radius in our model we calculate the distance between the center of mass of each aromatic ring and the center of mass of all aromatic rings in their respective pores.

The relative interlayer orientation was chosen based on clues from diffraction data as well as the various known stacking modes of benzene and substituted benzene rings: sandwiched, parallel-displaced and T-shaped [?] (Figures 3a to 3c).

- The T-shaped configuration was ruled out based on the inconsistency of its $\approx 5 \text{ \AA}$ equilibrium stacking distance [?].
- The system's preference towards the sandwiched vs. parallel displaced stacking modes will be explored.
- Both have reported stacking distances near 3.7 \AA
- Headgroups in the sandwiched configuration are stacked directly on top of each other while stacked headgroups in the parallel displaced configuration are offset by $180/n_{mon}$ degrees where n_{mon} equals the number of monomers per layer.

We tested a number of equilibration schemes of increasing complexity in an effort to match experiment while overcoming kinetic limitations that might trap the system in a metastable states. All start from an initial configuration generated with chosen structure variables.

- Equilibration Scheme A:
 - Steepest descent energy minimization
 - Short NPT simulation (5 ns) with berendsen barostat ($\tau_{barostat} = 1$) at 300 K
 - Switch to Parrinello-Rahman ($\tau_{barostat} = 10$) and run NPT simulation for 400 - 500 ns
- Equilibration Scheme B:
 - Restraints fix monomer head groups in the sandwiched or parallel-displaced configurations while allowing monomer tails to settle.
 - Doing so also mitigates system dependence on initial monomer configuration.
 - The restrained portion of the equilibration scheme is run in the NVT ensemble.
 - Every 50 ps, we reduce the force constants by the square root of its previous value, starting from $1\text{e}6 \text{ KJ mol}^{-1} \text{ nm}^{-2}$.
 - Once the force constant is below $10 \text{ KJ mol}^{-1} \text{ nm}^{-2}$, the restraints are slowly released until there is no more restraining potential.
 - The resulting unrestrained structure is allowed to equilibrate further in the NPT ensemble for 400 - 500 ns in the same way as Scheme A.
- Equilibration Scheme C:
 - A system equilibrated according to scheme B is cut in half so we can access longer simulation timescales
 - The system is simulated at 335K, close to its isotropic transition temperature, for 200 ns.
 - The structure is then linearly cooled back down to 300 K over 500 ns.
 - The system size is doubled back to its original size and equilibrated for 200 ns at 300 K.
 - Tried with and without an applied electric field.

- Equilibration Scheme D:
 - Even in the near dry Col_h system, there exists an equilibrium concentration of water.
 - The hydrogen bonding network formed by the water may play a role in structuring the pore.
 - We obtained an estimate of equilibrium pore water content by solvating an initial configuration with water baths above and below the membrane.
 - We ran the solvated system according to Scheme A but for 1000 ns
 - Using that number we added water to the pores of an initial configuration and equilibrated according to scheme B.

- In all cases, the v-rescale thermostat was used with tau-t = 0.1

Simulated X-ray diffraction patterns were generated based on atomic coordinates for a direct experimental comparison.

- All atomic coordinates were simulated as gaussian spheres of electron density corresponding to each atom's atomic number.
- A three dimensional fourier transform (FT) of the array of electron density results in a three dimensional structure factor which represents the unit cell in reciprocal space. z axis to generate a 2D cross section close to what one would see experimentally.
- We matched experimental 2D WAXS patterns by iterative improvement of our choice of initial structure and equilibration procedure.

We calculated ionic conductivity using two different methods for robustness.

- The Nernst-Einstein relation relates the DC ionic conductivity to ion diffusivity, D , concentration, C , ion charge, q , the boltzmann constant, k_b , and temperature, T :

$$\sigma = \frac{q^2 C D}{k_b T}$$

- Sodium ion diffusion coefficients were found by calculating the slope of the linear region of the mean square displacement curve as indicated by the einstein relation [?].
- We looked at the MSD plot to determine where to begin and end a linear fit
- Ion concentration was measured with respect to the entire unit cell.
- The second method, termed the 'Collective Diffusion' model, measures the movement of the collective variable, Q, which is defined as the amount of charge transfer through the system and can be thought to represent the center of charge of the system.
- The conductance, γ of the system can be calculated as:

$$\gamma = \frac{D_Q}{k_b T}$$

Conversion to ionic conductivity is achieved by multiplying by channel length and dividing by the membrane cross sectional area.

- D_Q is the diffusion coefficient of the collective variable Q. It can be calculated using the einstein relation.
- A full derivation of the model can be accessed elsewhere [?].

Using an equilibrated structure, a crosslinking procedure was performed in order to better parallel synthetic procedures.

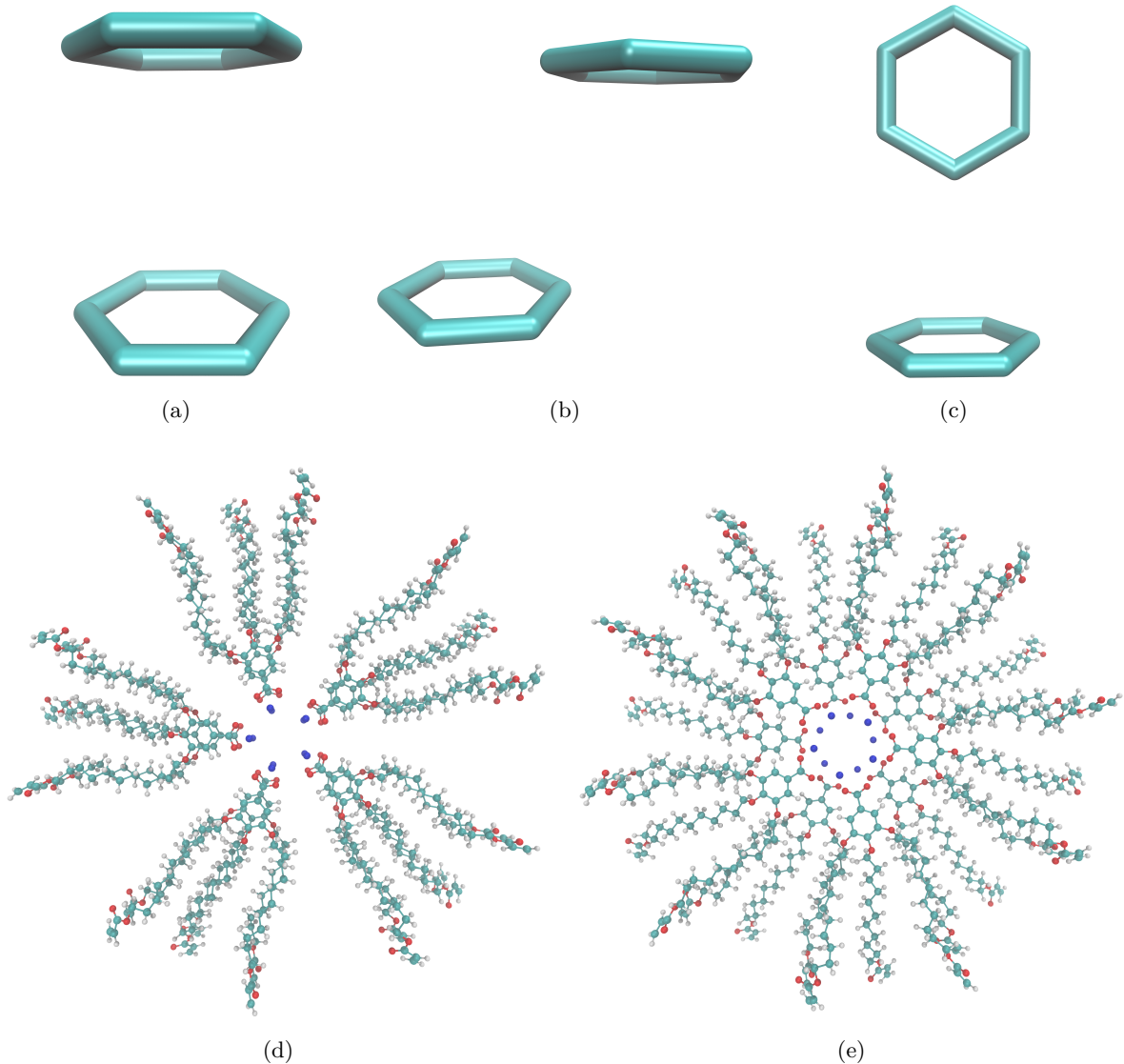


Figure 3: (a) Sandwiched benzene dimers stack 3.8 Å apart. (b) Parallel-Displaced benzene dimers stack 3.4 Å vertically and 1.6 Å horizontally apart. (c) T-shaped benzene dimers stack 5.0 Å apart. (d) Two monomer layers stacked in the sandwiched configuration (e) Two monomer layers stacked in the parallel-displaced configuration

- The purpose of crosslinking is to maintain macroscopic alignment of the crystalline domains, ensuring aligned, hexagonally packed pores.
- For that reason, we are not concerned with replicating the kinetics of the reaction, but instead emphasize the consistency of the final structure with experimental structural data.
- The algorithm was developed based on the known reaction mechanism.
- Crosslinking of this system is a free radical polymerization (FRP) taking place between terminal vinyl groups present on each of the three monomer tails.
- FRPs require an initiator which bonds to the system, meaning new atoms were introduced into the system.

- For simplicity, the initiator was simulated as hydrogen and made present in the simulation by including them in all possible bonding positions as dummy atoms.
- The crosslinking procedure is carried out iteratively.
- During each iteration, bonding carbon atoms are chosen based on a distance cut-off.
- The topology is updated with new bonds and dummy hydrogen atoms are changed to appropriate hydrogen types.
- Head-to-tail addition was the only propagation mode considered due to its dominance in the real system.
- Direction of attack was not considered because the resultant mixture is racemic.
- The resulting crosslinked structure has an even distribution of crosslinks between monomer tails of the same monomer, monomers stacked on top of each other and monomers in other pores, including across periodic boundaries.
- The pore spacing shrinks by $\approx 1 \text{ \AA}$ and stays constant under a range of simulation conditions.

Results and Discussion

Determination of Nanoscopic Structural Details

We will now address the questions raised in the introduction in the order that they were asked.

To discern the composition of the monomer layers, addressing (1), we ran simulations of systems created with 4 - 8 monomers per layer.

- Both the sandwiched and parallel displaced configurations were tested.
- All systems are stable after 400 ns of simulation.
- Table 1 shows the pore spacing for all systems tested.
- Systems built with 5 monomers in each layer equilibrate to a pore spacing that is most consistent with the experimental value of 4.12 nm derived from SAXS measurements (Figure 2a).
- The remainder of this discussion will focus on the analysis of systems built with 5 monomers per layer.

To answer (2), we verified that the system stays partitioned into layers by plotting the pair correlation function, $g(z)$ calculated between aromatic rings along the length of the pores (Fig 4).

- Sandwiched configuration layers stack 4.29 Å apart while parallel displaced configuration layers stack 4.37 Å apart. The power spectrums used to calculate the reported layer spacing are given in the Supplemental Information.
- Even though the layer spacing is similar, the sandwiched configuration exhibits more defined layers with its first peak deviating from the mean number density by 61 %.
- The parallel displaced configuration deviates from the mean by only 12 % in comparison.

The z -direction correlation functions show that layers in our model prefer to stack further apart than the 3.7 Å suggested by experiment. We attempted equilibration with layers stacked 4.0 nm apart and to our surprise, we observed long-term stability of a qualitatively different configurations suggesting that we have found more than one metastable free energy basin.

- Equilibrated systems built according to the 3.7 Å layer spacing implied by R- π are characterized by a defined, cylindrical and open pore structure.
- We will refer to this large set of configurations, with an open pore, as the OP Basin (open pore) (Figure 5a).

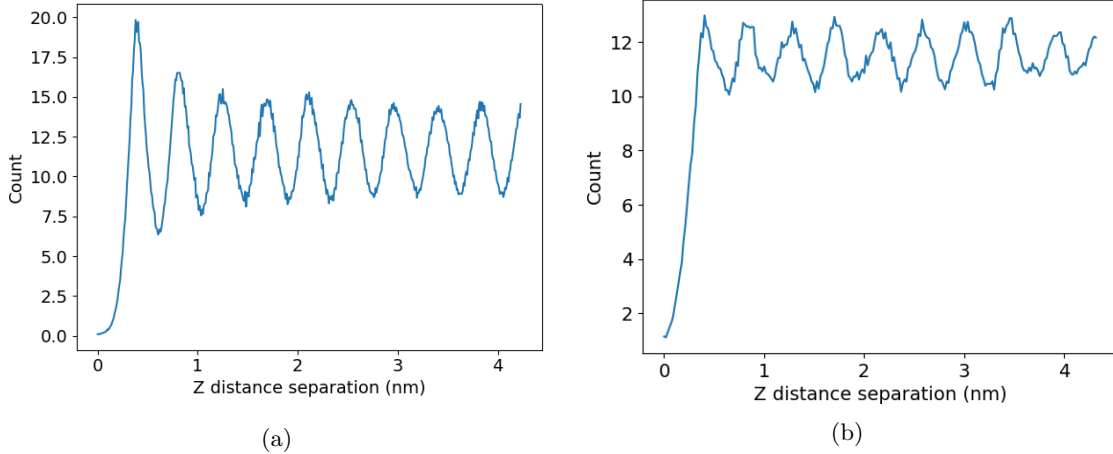


Figure 4: Pair distribution functions of aromatic carbons for the (a) 5 monomer per layer, sandwiched and (b) 5 monomer per layer, parallel displaced configurations. Clear periodic maxima in the z probability density indicate distinct layers. The magnitude of the spikes with respect to the average suggest that the 5 monomer per layer, sandwiched configuration possesses a higher degree of layer partitioning.

Monomers per layer	Starting Configuration	
	Sandwiched	Parallel Displaced
4	3.71 ± 0.04	3.84 ± 0.02
5	4.20 ± 0.04	4.23 ± 0.04
6	4.83 ± 0.03	4.85 ± 0.02
7	4.73 ± 0.03	4.84 ± 0.03
8	5.08 ± 0.04	5.46 ± 0.03

Table 1: The pore spacing (given in nm) of the model increases as number of monomers in each layer increases. The pore spacing of a system starting in the sandwiched configuration is systematically lower than that started in an offset configuration. Systems built with 5 monomers per layer in a parallel displaced configuration result in a pore spacing closest to the experimental 4.12 nm

- Simulations of systems built with layers stacked greater than 4 Å apart results in a pore structure characterized by high radial disorder, while still maintaining partitioning between hydrophobic and hydrophilic regions.
- This will be called the CP Basin (closed pore) (Figure 5b).
- This LLC membrane may exist in at least two metastable states.
- The distinct difference in pore structure exhibited by each phase will likely lead to different transport mechanisms.
- Because the pore structure will vary between each Basin, understanding which phase exists experimentally is necessary in order to ensure we are studying the system which actually dominates.

We answer question (3) by simulating X-ray diffraction patterns produced from equilibrated MD trajectories. We leave open the possibility that the experimental structure might be reminiscent of the parallel displaced or sandwiched configuration in the OP or CP basin.

- OP Basin systems were built in both the parallel displaced and sandwiched configurations with an initial layer spacing of 3.7 Å .

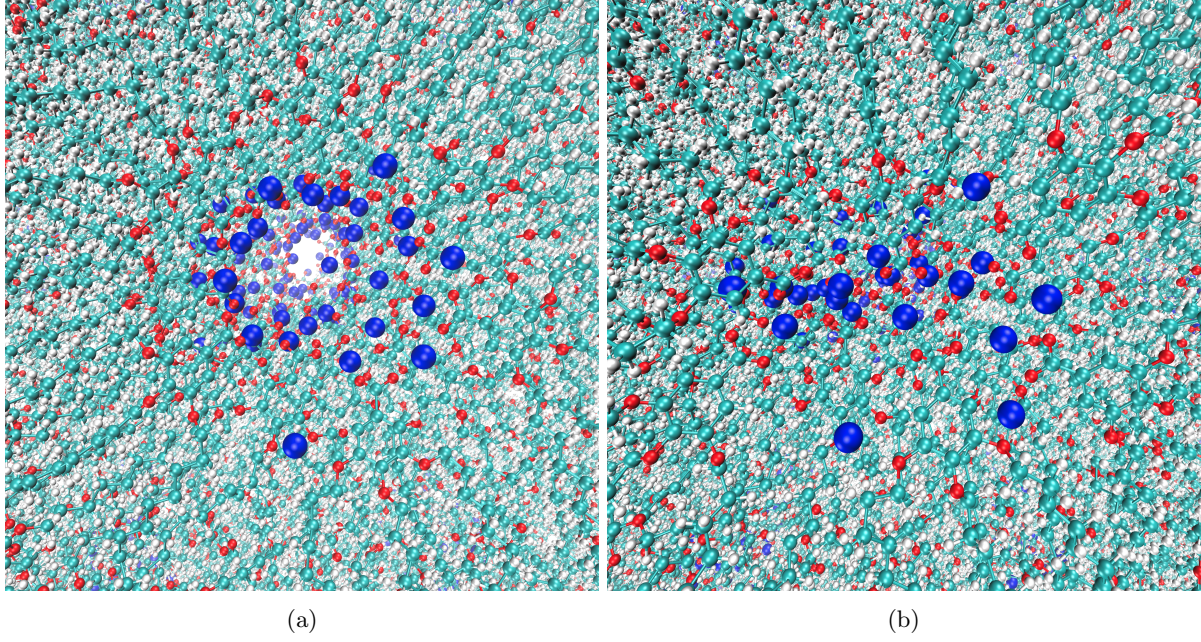


Figure 5: From a qualitative standpoint, the OP Basin (a) is characterized by a hollow cylindrical pore while pores in the CP Basin (b) are characterized by a higher degree of radial disorder

- A third system was created by stacking layers in the sandwiched configuration 5 Å apart in order to guide it towards the CP Basin.
- The three systems were equilibrated according to our procedure with NPT simulations of greater than 400 ns.
- Simulated diffraction patterns were generated using portions of the trajectory after equilibration.
- We assume the simulation has equilibrated when the distance between pores and the membrane thickness stopped changing.
- Simulated diffraction patterns for all three structures are shown in Figure ??.

Simulated diffraction of the disordered pore structure in the both the sandwiched and parallel displaced configurations does not match the experimental pattern.

- The disordered pore structure exhibits R-alkanes and R-pores but R-helix, R- π and R-spots are not present.
- Due to low resolution, making out the individual spots of R-pores is challenging and can be validated with slightly better resolution upon full spherical integration of the 3D structure factor. However, the same information can be extracted by measuring the pore spacing as described earlier.
- Although the structure's diffraction pattern is very different from experiment, its long-term stability suggests that the structure is realistic. We will explore this further when addressing (4).

Simulated XRD of the sandwiched configuration contains all experimental features except for R-helix.

- R-alkanes and R-pores appear in the expected locations.
- R- π is also present, intersecting R-alkanes at a lower q value than in experiment. The rings prefer to stack $\approx 4.1\text{\AA}$ apart as opposed to 3.7\AA .
- Most notably, R-spots appears in the expected location, which suggests that there is something intrinsic to closer packing that gives rise to such features.

The parallel displaced configuration results in a simulated XRD pattern with the closest match to experiment.

- It produces the only pattern that exhibits all major reflections
- R-alkanes, R-pores and R- π appear as they do in the sandwiched configuration.
- R-spots appears, however with a lower intensity relative to R-alkanes when compared to the sandwiched configuration.
- R-helix appears apparently due to the parallel displaced aromatic rings

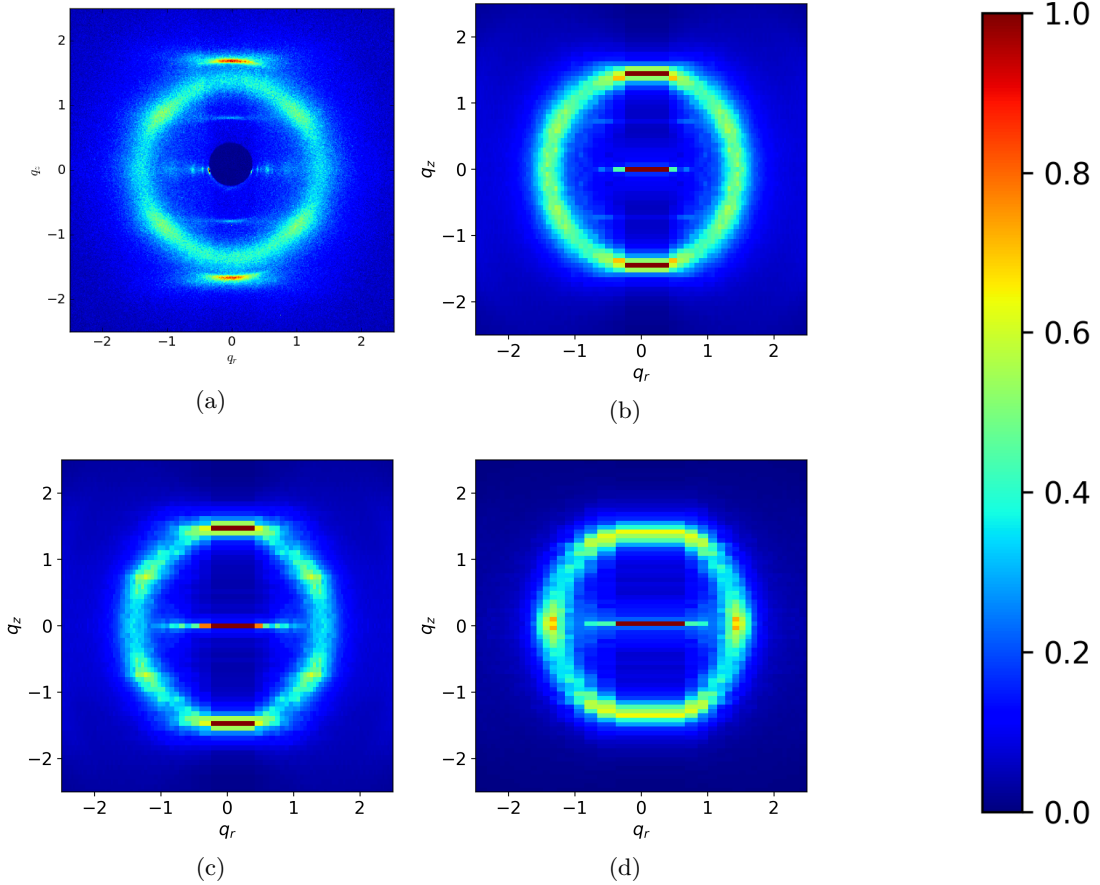


Figure 6: (a) Experimental 2D WAXS data contains 5 major reflections which we aim to match. The remaining three images are diffraction patterns simulated from MD trajectories. (b) The parallel displaced configuration gives rise to all reflections of interest. (c) The sandwiched configurations gives rise to a pattern with all major reflections except R-helix. R-spots is strong relative to R-alkanes in comparison to the parallel displaced configuration. (d) The disordered pore configuration creates a pattern with only R-alkanes and R-pores in common with experiment

R-spots appearing in the simulated XRD pattern of the OP basin conformations are a result of the way alkane tails pack together.

- Previously, the spots in the diffraction pattern had been explained as the product of tilted alkane chains.

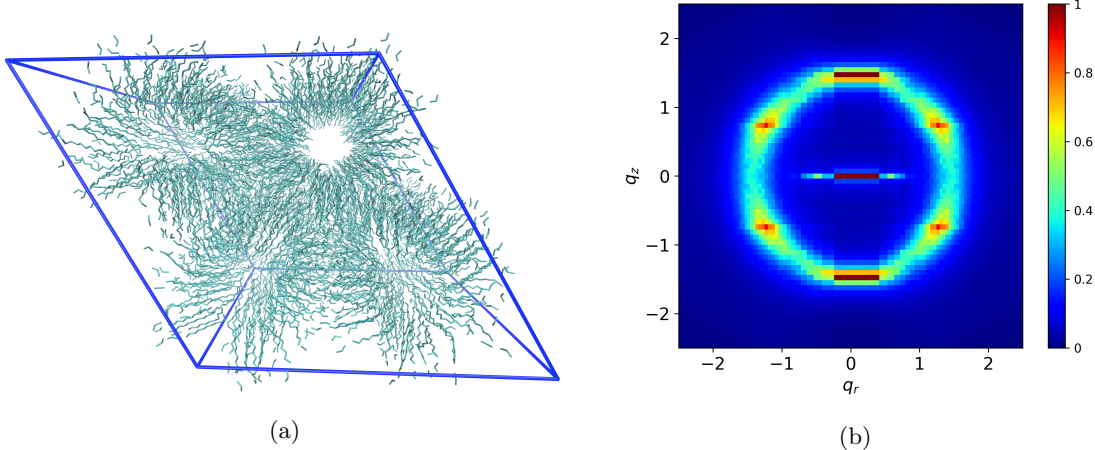


Figure 7: (a) All atoms except carbon atoms making up the tails are removed from the trajectory. (b) The simulated diffraction pattern of the tail-only trajectory still shows R-spots

- We measured the tilt angle of the alkane chains and showed that our system equilibrates to an average tilt angle close to zero degrees (See Supplemental Information).
- To understand the origin of the spots, we determined which atoms gave rise to the feature
- Since R-spots is present as higher intensity spots within R-alkanes, it is likely that the spots arise as a consequence of the tails.
- By removing atoms from the trajectory and simulating a diffraction pattern, we were able to isolate the cause of the spots to the tails (Figure 7).
- Since the tails stay nearly flat, we plotted the centroids of the tails and measured the angle between each centroid and its nearest neighbors with respect to the plane of the membrane (Figure ??).
- The distribution of these angles is consistent with the location of the spots (Figure 8).
- The peaks of interest in Figures 8a and 8b are located at $\pm 33^\circ$ which is the same location where the highest intensity of spots are located on the simulated patterns (See Supplemental Information for quantitative proof)
- We integrated the raw experimental 2D WAXS data in the region bounding R-alkanes and found the angle at which R-spots reaches its highest intensity to be $\pm 37^\circ$ which is a reconcilable difference with our simulated results.

The disordered basin shares little in common with the ordered basin but its long term stability suggests that it can exist under some conditions. We observed that Basin B is the dominant configuration at higher temperatures.

- We linearly ramped the temperature of a system in Basin A from 280K to 340K (just below the experimental isotropic transition temperature) over 100 ns.
- Visually, there is a distinct change in pore structure from one characteristic of the OP Basin (Figure 9a) to one characteristic of the CP Basin (Figure 9b).
- The slope of all order parameters changes between 315K and 325K (Figures 9c to 9e) indicating the possibility of an abrupt change in system ordering.
- Our 100 ns temperature ramp was likely too fast and caused the system to suffer from hysteresis.

We can not immediately classify the OP Basin and the CP Basin as separate phases.

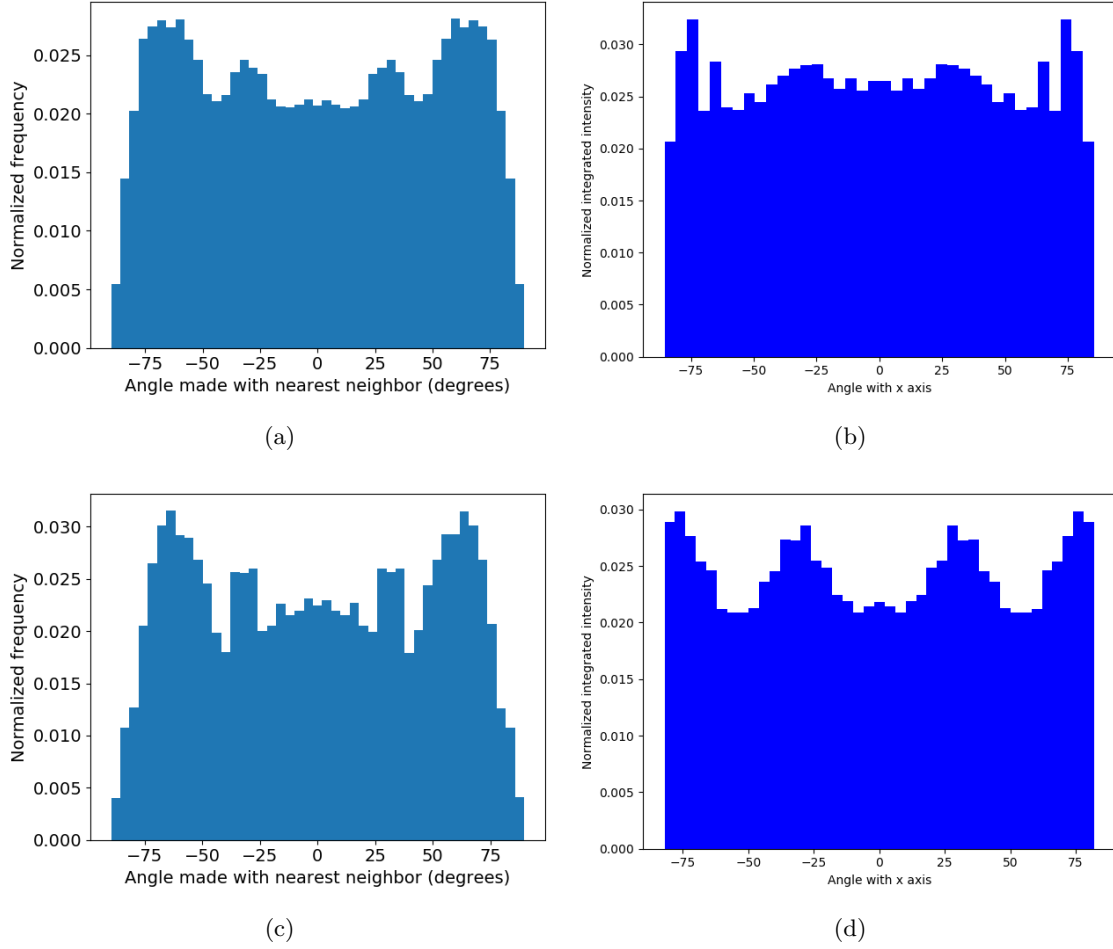


Figure 8: The distribution of angles w.r.t. the xy plane between alkane chain tail centroids and nearest neighbor centroids for equilibrated parallel displaced (a) and sandwiched (c) configurations. The same peaks are visible when the 2D simulated diffraction data is radially integrate in the R-alkanes region, (b) and (d) respectively.

- To prove the existence of two phases we need evidence of a first order phase transition.
- A first order phase transition can be denoted by a discontinuity of some order parameter in response to an external condition such as temperature.
- We chose three easily measurable order parameters: the distance between pores, the membrane thickness and the ratio of pore radius to the uncertainty in pore radius.
- The pore radius is divided by its uncertainty as a way of quantifying the degree to which monomers obstruct the pore region.

In an attempt to mitigate hysteresis, we performed slow, stepwise temperature ramps on a parallel displaced and a sandwiched configuration previously equilibrated at 300K.

- Every 200 ns, the temperature was raised 5K until we reached 345K
- We performed the same procedure with a system equilibrated in the CP Basin and used it as a benchmark for comparison.

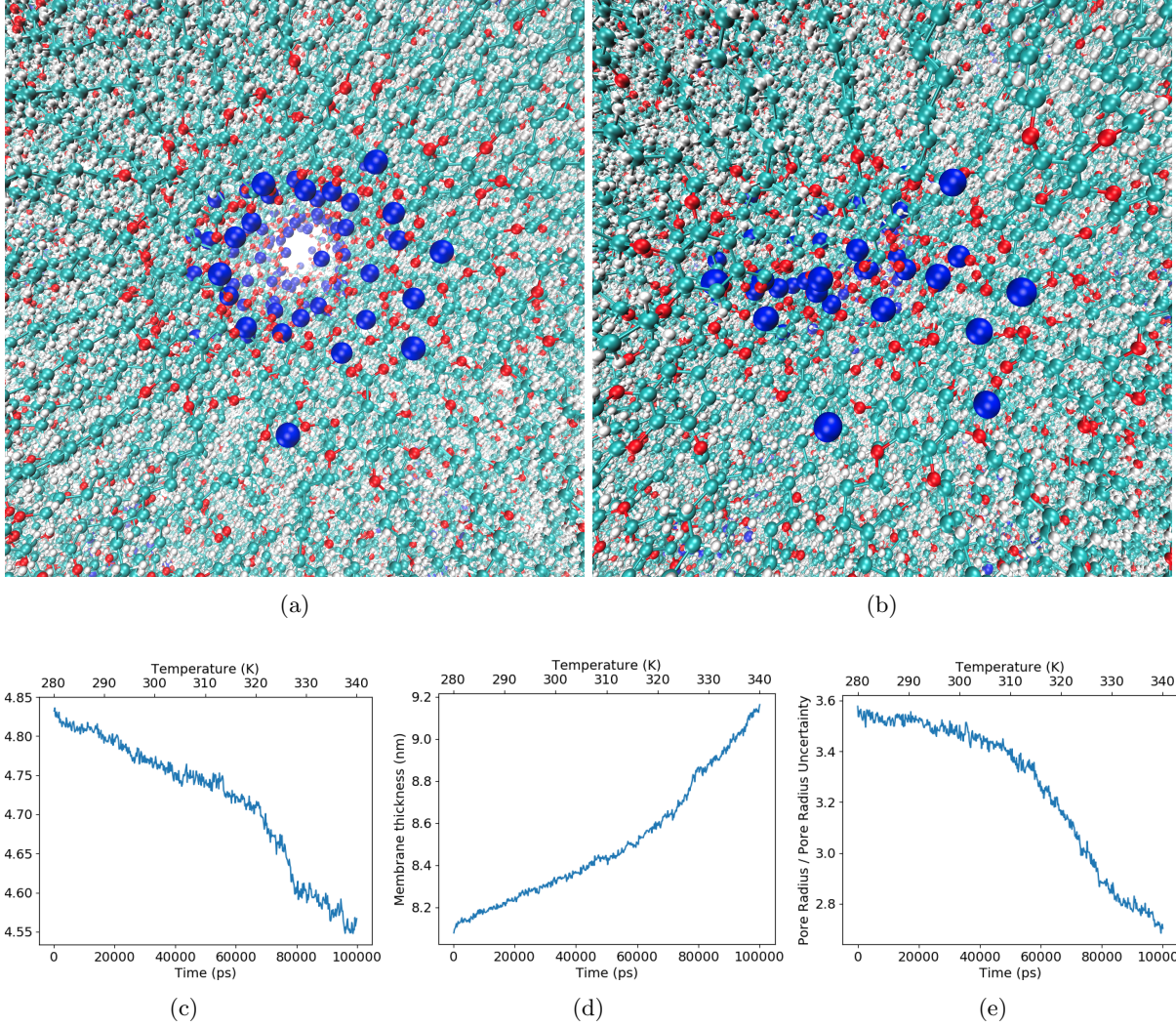


Figure 9: (a) The open pore structure exhibited by a structure equilibrated at 280K is characteristic of the OP Basin. (b) The closed pore structure with a high degree of radial disorder exhibited when the structure in (a) is heated to 340K is characteristic of the CP Basin. (c) A plot of distance between pores vs. temperature changes slope near 325K. (d) A plot of membrane thickness vs. temperature changes slope near 325K. (e) The plot of the ratio of pore radius to its uncertainty changes slope near 315K.

The CP and OP basins are two configurationally metastable basins.

- There is little change in CP basin properties during the temperature ramp.
- We observed smooth changes in order parameters as temperature of the OP Basin system was increased implying that we cannot claim the existence of two phases (Figure ??).
- Qualitatively, the pore structure of the OP basin system becomes comparable to one characteristic of the CP basin as temperature is raised. (?????)
- The OP basin system does not converge to the same order parameter values as the CP basin, however it is trending towards Basin B values. (??????)
- To resolve the quantitative discrepancy, we would need a slower temperature ramp
- Since there are no abrupt changes in any order parameter along the trajectory, we can conclude that the two basins are not separate phases

- The OP basin is the closest match to what is seen experimentally
- The CP basin is likely an intermediate between the Col_h phase and isotropic phase
- The CP basin is present in our simulations at lower temperatures than experiment because our model lacks sufficient $\pi\text{-}\pi$ interactions necessary to stabilize the system into the OP basin.

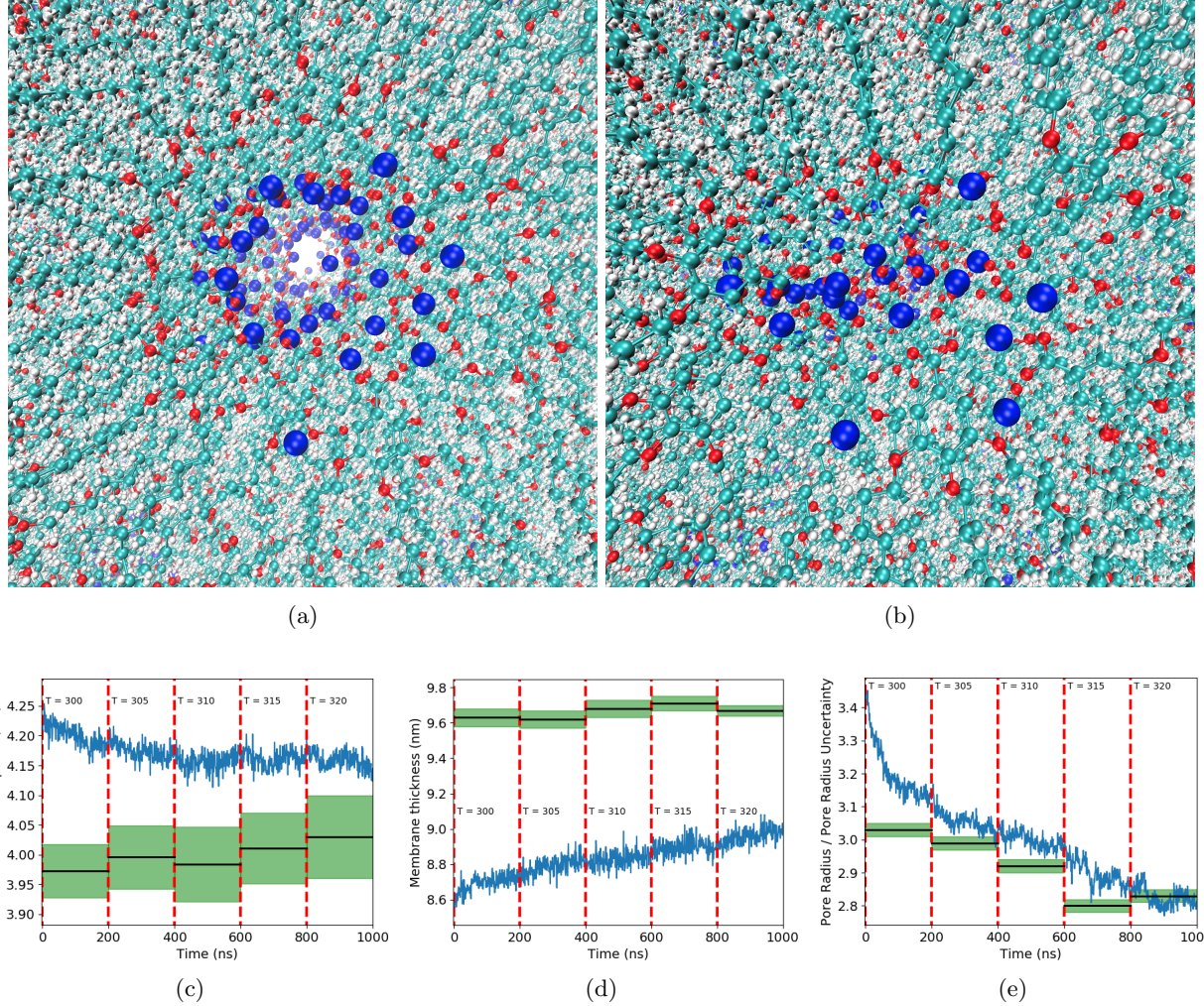


Figure 10: In all cases, blue lines represent the measured value of the order parameter, black lines are average values calculated from equilibrated Basin B systems at each temperature, green shaded regions represent the standard deviation of each of the black line values, and red dashed lines show where the temperature is bumped to the next level. (a) At 280K, the system is in a configuration reminiscent of Basin A. (b) At 335K, the system resembles a Basin B configuration. (c) The pore spacing of Basin A decreases with temperature approaching the value exhibited by Basin B. (d) The thickness of Basin A increases smoothly with temperature but is far from the Basin B value. Longer equilibrations at each temperature are needed to allow the system to fully expand. (e) The ratio of pore radius to uncertainty for Basin A changes smoothly with temperature, converging to a value below that exhibited by Basin B.

Ionic conductivity calculation

We use the equilibrated offset system in the OP basin to calculate ionic conductivity since its structure is the closest match to experiment. The model gives reasonable estimates of ionic conductivity when compared

to experiment.

- Calculated values of ionic conductivity obtained using the Nernst Einstein relation and Collective Diffusion model are compared in Table ??.
- The two methods agree with each other within error, although the uncertainty obtained using the Collective Diffusion model is much higher.
- Much longer simulations are needed to lower the uncertainty.
- Collective diffusion calculations were generated from 500 ns simulations.
- Our calculated values would benefit from longer simulations.
- For this reason we will likely only use the Nernst Einstein relation in future calculations of this type.

The CP basin has a higher ionic conductivity than the OP basin.

- We hypothesize that conductivity is enhanced in Basin B due to a higher sodium ion diffusivity.
- Transport of sodium is likely facilitated by the homogeneity of Basin B. Sodium ions have less nearby sites to move to in Basin A.
- There is currently no experimental evidence of this trend. Maybe Xunda will find something
- In both cases, our calculated values for Basin A are higher than the experimental values, as expected.
- Some of the discrepancy is likely a result of using an imperfect forcefield.
- However, the real system, although mostly aligned and straight, has a distribution of azimuthal angles, meaning that the pores have a degree of tortuosity which lowers the effective ionic conductivity of the bulk membrane.
- The ordering from isotropic to mostly aligned mesophases showed an 85 fold increase in ionic conductivity. We would expect additional gains in a perfectly aligned system.

	Calculated Ionic Conductivity Sm^{-1}	
Method	Basin A	Basin B
Nernst Einstein	1.23×10^{-4} (0.01)	1.76×10^{-4} (0.02)
Collective Diffusion	1.40×10^{-4} (0.32)	4.6×10^{-4} (2.4)
Experiment	1.33×10^{-5} (0.10)	—

Table 2: Calculated ionic conductivity using Nernst-Einstein and Collective Diffusion agree within error. Both methods give calculated values of ionic conductivity which are an order of magnitude higher than experimental values

Implementation of the crosslinking algorithm

We applied the crosslinking algorithm to the equilibrated sandwiched structure in the OP basin.

- There is an even distribution of crosslinks between same monomer tails, between monomers in the same pore and between monomers in different pores including periodic boundaries.
- We reach 95 % conversion of terminal vinyl groups
- The distance between pores shrinks by 1 Å after the system is crosslinked
- Major features are still present in the X-ray diffraction
- The ionic conductivity is higher/lower in the crosslinked system

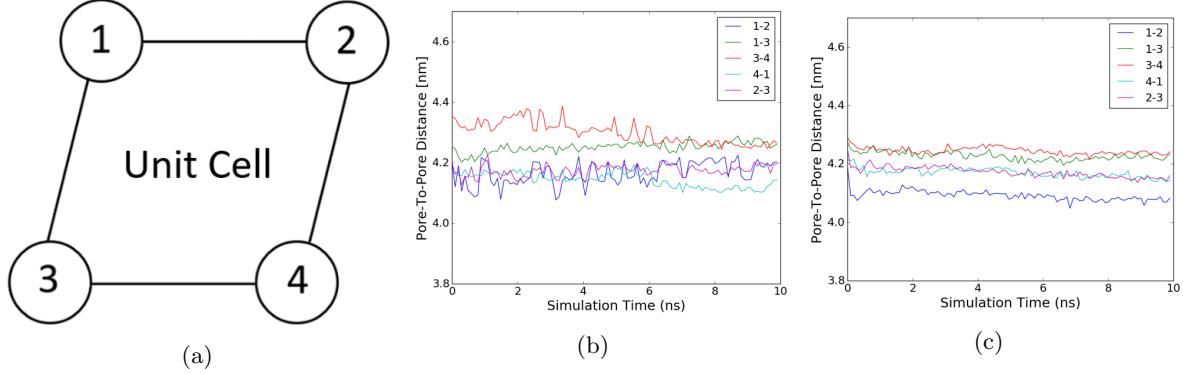


Figure 11: (a) The legends of the plots in (b) and (c) refer to the numbers shown. Each numbered circle represents a pore. Distances are measured along each of the lines shown in addition to the distance from pore 1 to pore 4. (b) The positions of individual pores fluctuate in an uncrosslinked system. (c) The positions of individual pores in the crosslinked system are stable relative to the uncrosslinked system

Conclusion

We have used a detailed molecular model of the Col_h phase formed by NA-GA3C11 in order to study the nanoscopic structure.

- While there have been efforts to model formation of various liquid crystalline phases with molecular dynamics, to our knowledge there have been no studies which attempt to examine their structure with the same level of detail presented here.
- We have confirmed that monomers stay partitioned in layers.
- We were able to deduce that layers are composed of 5 monomers.
- We have identified two metastable basins which each consist of a set of similar monomer configurations characterized by the degree of order in the pore region.
- We verified that the basins are not separate phases.
- We have explored the affect of two different $\pi-\pi$ stacking modes on the equilibrated membrane strucure.
- Simulated diffraction patterns generated from MD trajectories suggest that the offset configuration produces a structure with the closest match to experiment.
- Even though our model only answers these questions for a system created by NA-GA3C11, it can be adapted to other study systems formed by other LCs with little extra effort.